Journal of Physiology (1991), **436**, *pp.* 579–601
With 17 figures
Printed in Great Britain

CHARACTERIZATION OF ION CHANNELS SEEN IN SUBCONFLUENT HUMAN DERMAL FIBROBLASTS

BY MARK ESTACION*

From the Department of Physiology and Biophysics, University of California, Irvine, CA 92717, USA

(*Received 13 July 1990*)

SUMMARY

1. Ion channels expressed in human dermal fibroblasts are characterized using the patch-clamp technique.

2. A number of different ion channels were found but their expression occurred at various frequencies. The most commonly found phenotype was the expression of voltage-gated K^+ current. This 'typical' K^+ current was seen in about 60% of the cells recorded.

3. Subtypes of voltage-gated K^+ channels could be discerned by differences in gating kinetics. One has fast inactivation and resembles the 'A' K^+ current. Additional subtypes were sometimes discerned based on activation kinetics.

4. The large-conductance Ca^{2+}-activated K^+ channel (maxi-K^+) could be found in nearly every cell but required large depolarizations to activate using the standard Ca^{2+}-buffered pipette solution (10^{-8} M $[Ca^{2+}]_i$).

5. Inward rectifier K^+ channels were seen in a low percentage of cells. The inward rectifier K^+ current was sensitive to 'wash-out' if guanosine 5'-*O*-(3-thiotriphosphate) (GTPγS) was included in the pipette solution dialysing the cell.

6. Tetrodotoxin (TTX)-sensitive voltage-gated Na^+ channels were seen but in a lower number of cells recorded, about 20%. Evidence for subtypes of Na^+ channels were sometimes seen based on differences in gating kinetics.

7. An ATP-dependent osmotically activated Cl^- current was also found. This current showed some outward rectification but was otherwise voltage independent.

8. In addition, a cell-to-cell contact-associated K^+ current was described. This current was linear over the voltage ranges used and whose gating correlated with the existence of gap junctions.

9. These currents were characterized to determine the baseline behaviour of unstimulated cells and to compare to bradykinin-stimulated cells described in the following paper. As unexcitable cells, human dermal fibroblasts are capable of expressing a surprising diversity of ion channel phenotypes and of ion channel modulations.

* Present address: Cancer Research Center of Hawaii, 1236 Lauhala Street, Honolulu, HI 96813, USA.

INTRODUCTION

Fibroblasts have been used as a model system for many biochemical and physiological processes, primarily because they grow well in culture and are one of the few sources of human tissue routinely available for clinical and basic research. Much is known about their growth characteristics in culture and about the biochemical events associated with growth stimulation and transformation. However, little is known about ion channels in fibroblasts.

Before the advent of patch-clamp recording (Hamill, Marty, Neher, Sakmann & Sigworth, 1981), only microelectrode recordings had been attempted on fibroblasts. No evidence for excitable behaviour was found and the potentials reported were compromised due to the difficulty of recording from very small cells (Lamb & MacKinnon, 1971; Yen-Chow, Chow, Jee & Woodbury, 1984). Even at this stage, however, Ca^{2+}-activated K^+ channels were hypothesized to account for the spontaneous hyperpolarizations seen in L cells, a mouse fibroblastic line (Okada, Tsuchiya, Yada, Yano & Yawo, 1981; Ince, Leijh, Maijer, VanBavel & Ypey, 1984).

The existence of ion channels in fibroblasts was also hypothesized from flux measurements. The presence of Na^+ channels was postulated because of specific TTX binding and the ability of veratridine, a scorpion toxin which opens Na^+ channels, to cause increased Na^+ flux (Munson, Westermark & Glaser, 1979; Lombet, Frelin, Renaud & Lazdunski, 1982). Direct observation of ion channels in fibroblasts, however, did not occur until the advent of the patch-clamp technique.

Since fibroblasts are being used to study very important physiological processes, including growth regulation, learning more about their general physiology is important. The reports describing increases in ion fluxes in response to growth factor stimulation suggested that ion channels might be involved. Thus a survey of the electrophysiological properties of human fibroblasts was undertaken with the hope of finding growth factor-modulated ion channels.

This paper characterizes ion channels found in human skin fibroblasts. Using both whole-cell and single-channel recording, several distinct types of voltage-dependent and voltage-independent channels are described. The culture conditions and morphology of the cells are noted to detect any correlations of ion channel expression with the state of the cell. Possible roles for some of the ion channels are discussed. The characterization of the ion channels normally found in the fibroblast defines a baseline from which to detect mitogen-stimulated modulation described in the accompanying paper (Estacion, 1991). This paper includes currents characterized while performing control experiments for the addition of nucleotides to the pipette solutions used in the companion paper. While this is a comprehensive report of all the ion currents found to date, human fibroblasts will probably be found to express even more types of ion currents in the future.

METHODS

Cell culture

Stocks of human dermal fibroblasts, derived from primary culture of newborn foreskin explants donated locally, were generously supplied by Dr Harry Haigler (Department of Physiology and Biophysics, University of California, Irvine) and Dr Dennis Cunningham (Department of

Microbiology and Molecular Genetics, University of California, Irvine). Serial cultures were grown on untreated sterile plastic flasks (Costar) and passed (1:5) using brief trypsinization. These primary cultures exhibit reduced growth rates and morphological changes occurring after passage 13 or 14. Experiments were performed on cells at passage 4 through 16 but usually on cells between passage 8 and 12. Electrophysiological experiments were done on cells plated onto untreated circular glass cover-slips which were placed into the wells of a 24-well culture plate (Costar). The cells were plated at low density so that cells would remain isolated and were grown for at least 24 h in order for the cells to attach and reattain fibroblast morphology. The cultures were maintained in complete medium (described below) in a humidified 5% CO_2 incubator at 37 °C. Immediately before recording, the cover-slip was transferred to a perfusable chamber mounted on the stage of an inverted microscope.

Culture media. Experiments were performed with cells grown using either Dulbecco's modification of Eagle's medium (DMEM; Mediatech, Washington, DC) or Alpha modification of Eagle's medium (αMEM; Mediatech). No differences in the range or distribution of currents expressed was noted using either medium. Growth curves showed that the doubling rate and the saturation density was slightly higher for cells grown in αMEM. The pH buffering seemed better in αMEM also and for these reasons αMEM was preferred slightly. Growth in a defined, serum-free medium was attempted (EX CELL 300; JR Scientific, Woodland, CA, USA) but the cells grew poorly with little ion channel expression and thus was discontinued.

Serum. Complete medium contains 10% fetal bovine serum, 1% glutamine, and no antibiotics. New serum lots were tested for their effects on growth and electrophysiological properties, since it was noted that these properties could change depending on the serum manufacturer and lot number. During the course of these studies, the following sera were used: Hyclone (Ogden, UT, USA). Rehatuin (Armour Pharmaceuticals) and JR Scientific (Woodland, CA, USA). All sera contained low levels of endotoxin and were hybridoma-tested.

Solutions and reagents

Bath solutions. The standard recording solution was mammalian Ringer solution. It consists of (in mM): 160 NaCl, 4·5 KCl, 2·0 $CaCl_2$, 1·0 $MgCl_2$, and 5 HEPES. External solutions were titrated to pH of 7·2 with NaOH and have measured osmolarities of 290 to 320 mosM. Solutions used for determining cation permeability were formed by substituting the test cation for Na^+. *N*-Methyl-glucamine (NMG), tetramethylammonium (TMA), choline, K^+ and Cs^+ Ringer solution are examples. Solutions used to determine anion permeability were formed by substituting the test anion for Cl^-. Sodium aspartate Ringer solution and sodium propionate Ringer solution are examples. Ba^{2+} Ringer solution, used to evaluate divalent permeability, is composed of 104 mM-$BaCl_2$, 1·0 mM-$MgCl_2$ and 5 mM-HEPES. Most pharmacological agents were prepared as 100× stock solutions in distilled water then frozen in aliquots. On the day of the experiment, the aliquot was diluted to the desired concentration in mammalian Ringer solution for use. Tetrodotoxin (TTX), (Calbiochem), charybdotoxin (CTX), (gift from Chris Miller), ionomycin (Calbiochem), bradykinin (Calbiochem), and apamin (Sigma) were all handled in this manner. Tetraethyl-ammonium (TEA) (recrystallized, Sigma) and 4-aminopyridine (4-AP) (recrystallized, Sigma) solutions were made directly in mammalian Ringer solution. In order to vary the external K^+ concentration, K^+ Ringer solution was diluted with Na^+ Ringer solution. This allowed the exchange of Na^+ for K^+, while maintaining constant pH and osmolarity.

Pipette solutions. The standard pipette recording solution was composed of (in mM): 160 potassium aspartate, 2·0 $MgCl_2$, 1·1 K_2EGTA, 0·1 $CaCl_2$, and 10 HEPES. The calculated free Ca^{2+} level is 10^{-8} M. The pH was adjusted to 7·4 and the osmolarity ranged between 290 and 320 mosM. Internal solutions containing nucleotides were made by adding the sodium salt of GTP, ATP, or GTPγS (Boehringer Mannheim) to the potassium aspartate internal solution and frozen into aliquots. For each day of experiments, a fresh aliquot was thawed for use.

Electrophysiology

Patch-clamp experiments were performed as described by Hamill, Marty, Neher, Sakmann & Sigworth (1981). Pipettes were pulled using soft glass (Accu-fill) and coated with Sylgard (Dow Corning) with resistances in the range of 1–10 Ω. The current was measured with a LIST L/M-EPC-7 amplifier (Darmstadt, Germany) which allowed for compensation of cell capacitance and series resistance. The signal was then passed through an eight-pole Bessel filter (Frequency Devices,

Haverhill, MA, USA), usually at 3000 Hz, before digitization and computer storage. For single-channel recording of long continuous records, the signal was routed to a PCM processor (Sony) and then stored on videotape.

The interface for computer-controlled pulse stimulation, digitization, and storage of the resultant current was built from a design by Dr F. Bezanilla at UCLA. The 12-bit A/D converter is capable of sampling at 400 kHz. The interface communicates with an IBM PC-AT microcomputer using programs written in FORTRAN.

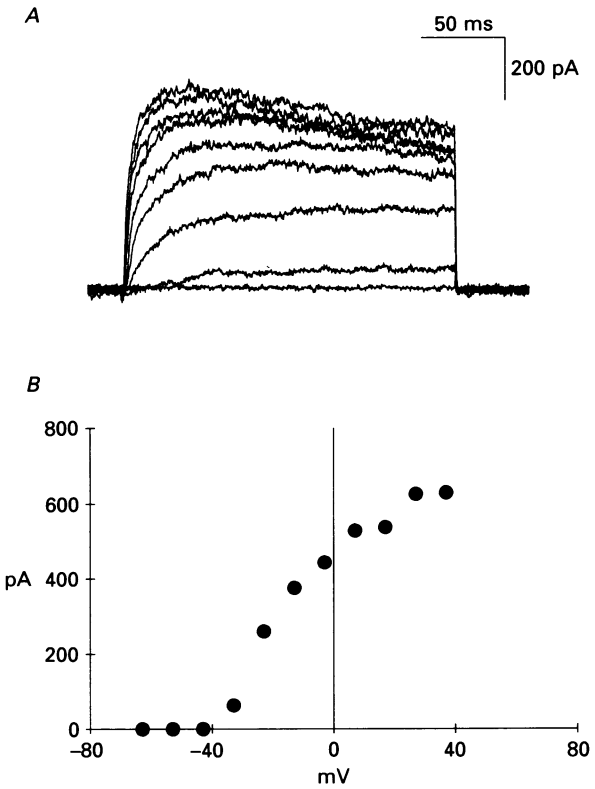

Fig. 1. 'Typical' K^+ currents. *A*, whole-cell currents from human fibroblasts elicited by 200 ms depolarizing pulses from a holding potential of −93 mV to the values −63 to 47 mV in 10 mV increments. Linear currents have been subtracted using a P/4 protocol in the range of −120 to −90 mV. Cell was bathed in mammalian Ringer solution and the pipette solution was standard potassium aspartate with 0·3 mM-GTP added. *B*, current–voltage relation for 'typical' K^+ current. ●, the peak values during the pulses for the traces shown above.

The programs for pulse stimulation and data acquisition are capable of several pulse protocols, including leak subtraction using the P/4 protocol (Armstrong & Bezanilla, 1974) and ramp stimulation. Pulse protocols can be named and stored so that identical experiments can be performed on demand. The pulse protocols used to distinguish and characterize ion channels are thus identical between different cells, and allows for the statistical comparison of the hundreds of cells recorded.

RESULTS

Voltage-gated channels

K^+ channels

The pattern of currents most often observed is illustrated in Fig. 1. These outward currents show kinetics similar to delayed rectifier K^+ currents (Fig. 1*A*) with no

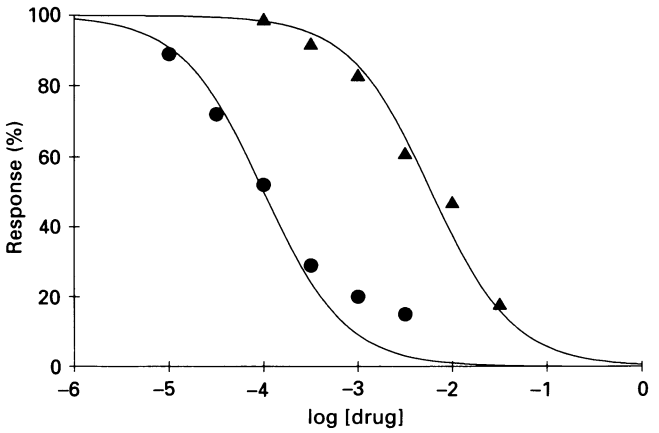

Fig. 2. Pharmacological properties of 'typical' K^+ current. Dose–response curves to both 4-AP and TEA were performed by measuring the response to a pulse to 17 mV at the drug concentrations indicated and normalizing to control responses recorded from the same cell. These values were plotted *vs.* the log of the drug concentration. Both data sets were measured in the same cell. The pipette contained standard potassium aspartate. The lines are binding curves fitted by eye to the data. The K_d (dissociation constant) values predicted are 100 μM for 4-AP (●) and 6 mM for TEA (▲).

discernable tail currents at the repolarization potential of −93 mV. The filled circles represent the peak currents measured from the sweeps in Fig. 1*A* plotted *versus* the pulse potential, generating the peak-current–voltage (*I–V*) curve. The K^+ current shows inactivation during the pulse at the larger pulse potentials. Recovery from inactivation was slow and full recovery from inactivation required tens of seconds (data not shown).

Some pharmacological properties of this current are shown in Fig. 2. The dose–response curves to the K^+ channel blockers, TEA and 4-AP, are shown with apparent K_d (dissociation constant) values of 6 and 0·1 mM respectively. The reversal potential of the current shifts with changes in external $[K^+]$ as predicted by the Nernst equation (data not shown). Using the three characteristics of ion selectivity, gating and pharmacology, these currents are identified as voltage-dependent K^+ currents.

Variability in kinetics was noted between cells suggesting that the macroscopic K^+ current might be composed of multiple populations of K^+ channels. Support for this hypothesis comes from rare cells which seem to predominantly express a single

population of K^+ channel. At least one but possibly three subtypes of voltage-dependent K^+ channels could be inferred by differences in kinetics. Some cells also showed multiple kinetic components which could be described as the sum of currents identified and described below.

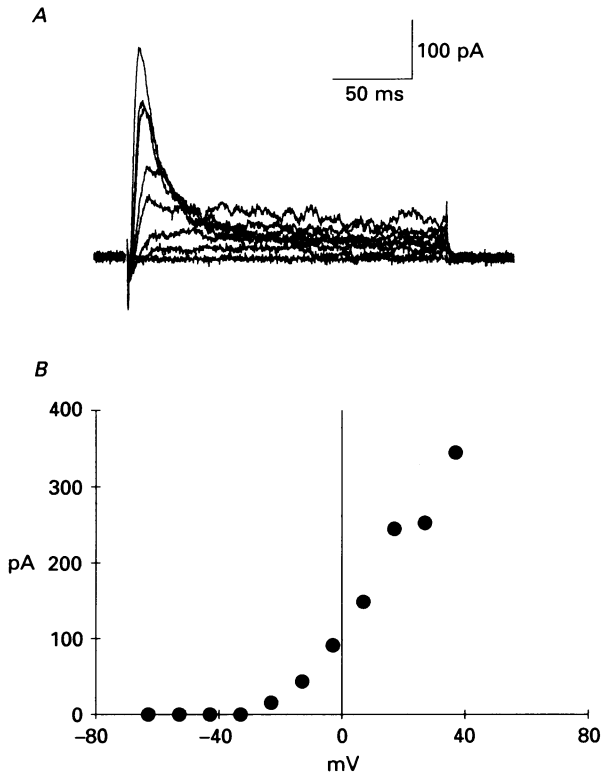

Fig. 3. 'A' K^+ currents. *A*, whole-cell currents elicited by a series of 200 ms depolarizing pulses as described in Fig. 1. Note the fast inactivation of the outward current during the pulse. Cell was bathed in mammalian Ringer solution and the pipette contained standard potassium aspartate solution. *B*, current–voltage relation obtained from peak currents during the pulses shown above.

The most discernable kinetic behaviour was the expression of a quickly inactivating current which might be termed an 'A' K^+ current (Connor & Stevens, 1971). The fast inactivation during pulses is clearly evident from the records shown in Fig. 3*A*. While the current inactivates quickly during the pulse it also recovers quickly upon repolarization. Significant expression of the 'A' K^+ current was rare, less than 5% of cells, but its distinctive properties allowed it to stand out when it was observed.

Two kinetic variants of the 'typical' K^+ current were also consistently seen at low frequencies. The first was dubbed 'late' because of an activation curve which was shifted about 20 mV more positive. This current showed no inactivation during the

pulse and recovered quickly upon repolarization (data not shown). The other was dubbed 'slow' because the current rose slowly during the pulse, often failing to peak within the 200 ms pulse duration. While inactivation was not clearly evident during the standard 200 ms pulse, this current recovered slowly upon repolarization (data

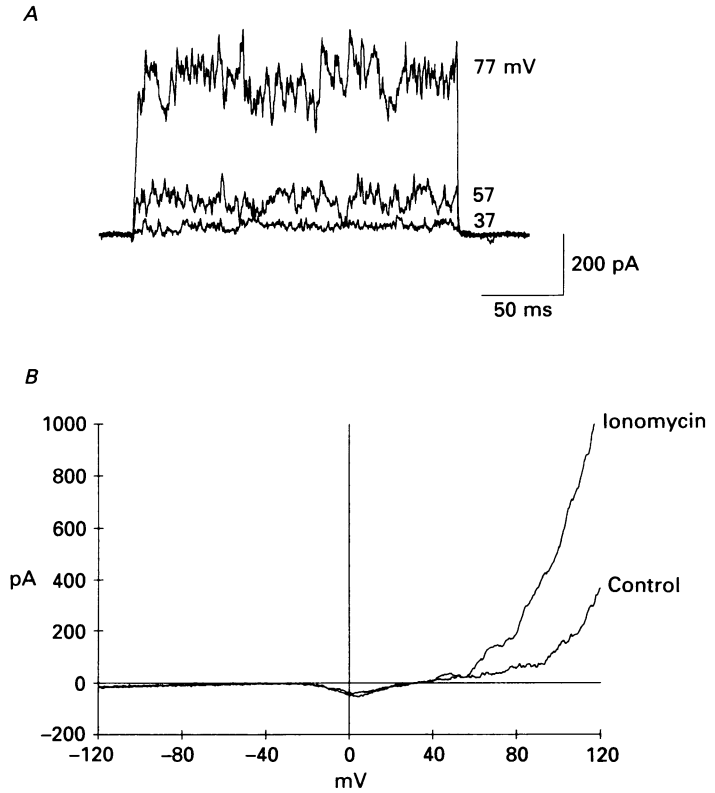

Fig. 4. Ca^{2+}-activated K^+ current (maxi-K^+). *A*, whole-cell currents measured in response to pulses with the potentials indicated. This cell had essentially no other ion channels activated by voltage. The bath solution was mammalian Ringer solution and the pipette contained standard potassium aspartate. Note the increased activity of very noisy outward currents at the large stimulus potentials. *B*, whole-cell ramp currents obtained in control and in the presence of 1 μM-ionomycin. The ramp waveform consists of a smoothly varying command voltage which spans the voltage range indicated over a 100 ms duration. Note that the range of the ramp continues to +120 mV and the outward rectification is not seen until above +40 mV. These records, which are from a different cell from part *A*, also expressed voltage-gated Na^+ current, indicated by the small inward deflection centred around 0 mV. The pipette solution contained potassium aspartate with no added nucleotides.

not shown). The identification of these kinetic variants in terms of their underlying ion channels remains to be done.

An additional voltage-dependent K^+ current can be seen at very large depolarizations. The sweeps shown in Fig. 4*A* in response to pulses of large potentials

exhibit large fluctuating outward current. Note that this current is not significantly active below +40 mV and thus is not detected with the standard pulse protocols. Experiments using the Ca^{2+} ionophore ionomycin are described in the companion paper to cause a rise in intracellular calcium concentration . Exposure of a cell

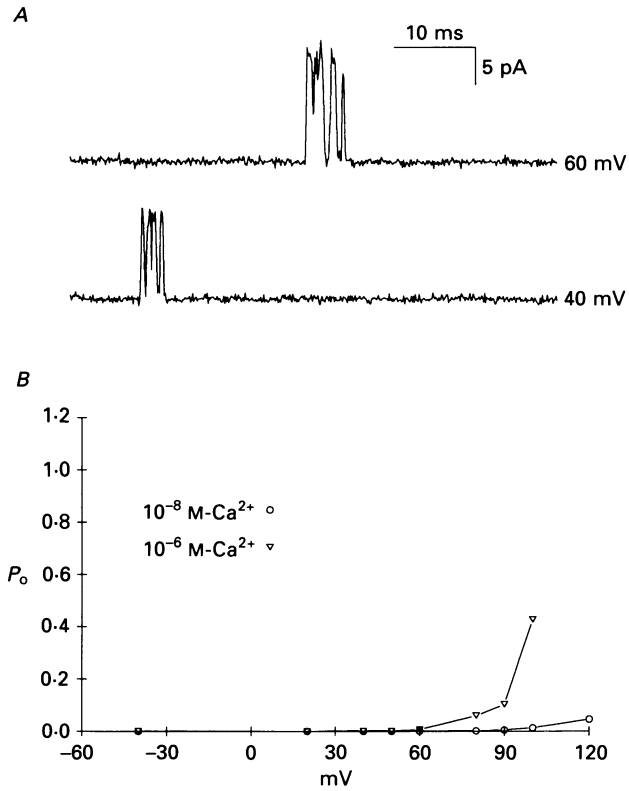

Fig. 5. Ca^{2+}-activated maxi-K^+ single channels. *A*, single-channel activity recorded from an outside-out patch at the potentials indicated. The pipette contained standard potassium aspartate. Well-resolved openings of a large (approximately 120 pS) K^+ channel are shown. Note also that these voltages do not elicit frequent openings. *B*, probability of opening *vs.* voltage curves were constructed from a different patch pulled in the inside-out configuration allowing the bath exchange of buffered low-Ca^{2+} solutions to determine the sensitivity of the fibroblast maxi-K^+ channels to calcium. The pipette contained mammalian Ringer solution and the solutions applied to the cytoplasmic face of the patch were KCl solutions buffered to various calcium levels with EGTA. Segments of steady-state recordings (10 s) were idealized using 50% threshold detection and the resulting summed open time was divided by the total time analysed to yield the probability of opening (P_o).

containing this outward current to ionomycin caused a shift in the activation towards less depolarized (but still very large) potentials. Figure 4*B* shows the current response to a ramp stimulus before and after applying 1 μM-ionomycin. The sensitivity of this current to block by TEA (1 mM) and CTX (100 nM) (data not

shown) argue that this current is probably carried through 'maxi-K^+' Ca^{2+}-activated K^+ channels.

Further support for this conclusion comes from single-channel recordings which show a large conductance (120 pS) K^+ channel (Fig. 5*A*). The voltage dependence at

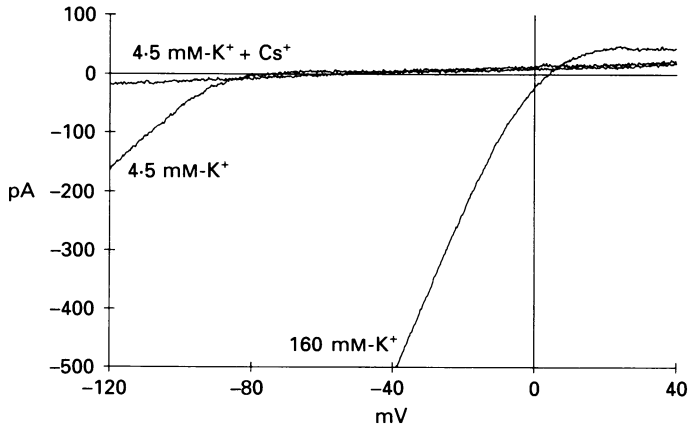

Fig. 6. Inward rectifier K^+ current. Whole-cell currents elicited using a ramp stimulus showing characteristic inward rectifier K^+ currents. The sweep marked 4·5 mM-K^+ is taken in mammalian Ringer with the pipette containing potassium aspartate. Switching to K^+ Ringer, marked 160 mM-K^+, causes the inward rectification to shift approximately 80 mV to near 0 mV. Addition of 16 mM-Cs^+ to mammalian Ringer solution caused a near total block as shown.

two levels of intracellular $[Ca^{2+}]_i$ of the probability of opening for a single channel was constructed (Fig. 5*B*). The potential range at which the maxi-K^+ channels activate suggests that they underlie the currents seen in Fig. 4. These maxi-K^+ channels were expressed in every cell in which large depolarizations were attempted in whole cell, and could be seen in nearly every outside-out patch pulled, suggesting a large and constitutive expression of these channels in human fibroblasts.

Human fibroblasts can also express inward rectifier K^+ current similar to that described in muscle (Adrian & Freygang, 1962). The current is seen as inward rectification in ramps (Fig. 6) when the applied potential is lower than the Nernst potential for potassium. The dependence on extracellular $[K^+]$ is clearly shown by shifts in reversal potential of the current (Fig. 6), characteristic of the inward rectifier. Another characteristic of the inward rectifier K^+ current is block by extracellular Cs^+ (Fig. 6). The expression of inward rectifier showed evidence for dependence upon serum source, being reliably expressed with some sera while rarely with others.

Experiments performed with GTPγS included in the pipette are described in the accompanying paper (Estacion, 1991). In cells that expressed inward rectifier, however, it was noticed that the inward rectifier current seemed to consistently 'wash-out' ($n = 14$) over a period of minutes. An example is shown in Fig. 7. After a lag period, the quantified inward rectifier conductance decreases linearly until it is

completely abolished (Fig. 7*B*). The current was abolished only when GTPγS was included in the pipette and not when control potassium aspartate or potassium aspartate with added ATP or GTP was used (data not shown).

Na^+ channels

Voltage-dependent inward currents could often be recorded from human fibroblasts as shown in Fig. 8. Depolarizing pulses result in a quickly activating

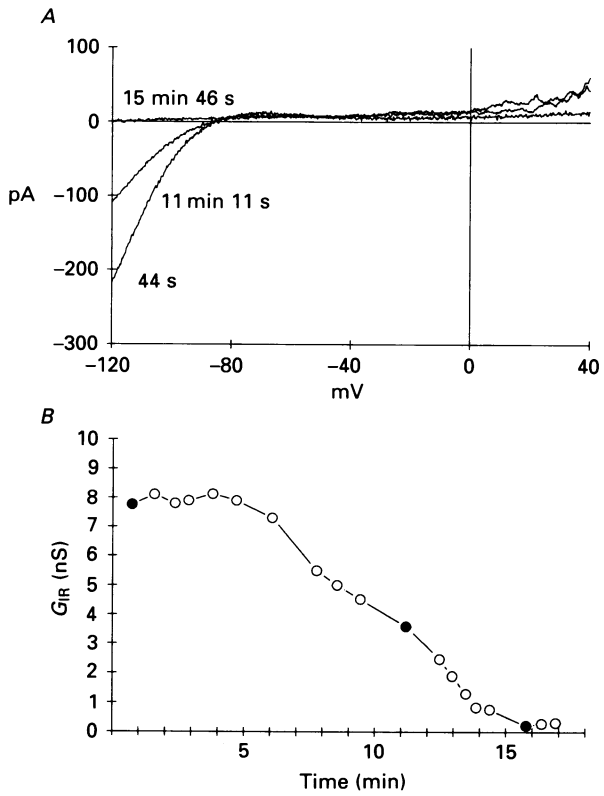

Fig. 7. GTPγS-induced wash-out of inward rectifier. *A*, ramp currents taken at various times after establishing the whole-cell configuration. The pipette solution, which was composed of standard potassium aspartate with 100 μM-GTPγS added, dialysed the cell. The bath solution was mammalian Ringer solution. *B*, slope conductance measured between −110 and −90 mV quantifying the inward rectifier K^+ current (G_{IR}) is plotted as a function of time since break-in. ●, data traces shown in part *A*.

inward current which subsequently inactivates (Fig. 8*A*). The current is reversibly abolished if the external Na^+ is exchanged with TMA or NMG (data not shown). The kinetics and ionic dependence are characteristic of current through voltage-dependent Na^+ channels. The *I–V* relation determined from the pulses (●) is shown in Fig. 8*B*.

This current is also sensitive to TTX, a blocker specific for voltage-dependent Na^+

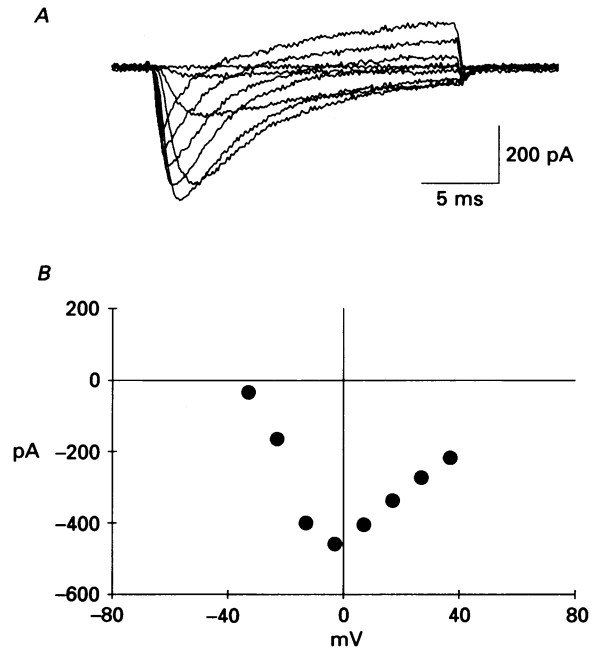

Fig. 8. Voltage-dependent Na^+ current. *A*, whole-cell inward currents elicited by 20 ms depolarizing pulses. The pulse protocol included a 50 ms pre-pulse to −110 mV to remove inactivation and P/4 leak subtraction. Series resistance compensation was employed to reduce voltage error during the responses. Bath solution was mammalian Ringer solution and the pipette contained standard potassium aspartate. *B*, current–voltage relation measured from the peaks during pulses shown above.

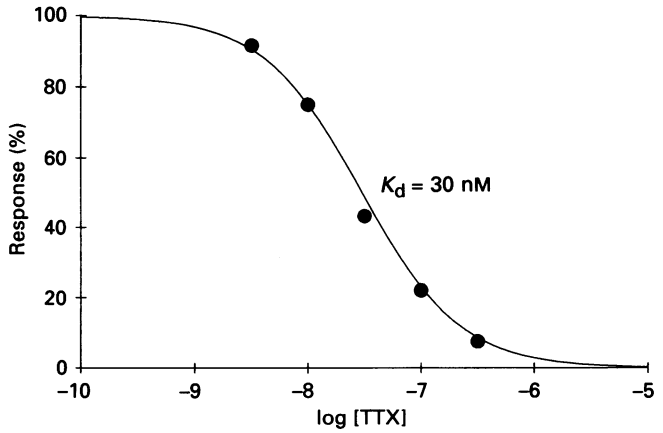

Fig. 9. Na^+ current TTX dose–response. The TTX dose–response curve generated by the normalized responses of the Na^+ current in the presence of various concentrations of TTX solubilized in mammalian Ringer solution. The pipette contained standard potassium aspartate with 0·3 mM-GTP added. The binding curve represents a fit by eye with the K_d value shown.

channels. The TTX dose–response curve is shown in Fig. 9. The apparent K_d of 30 nM is typical for fibroblast Na^+ channels ($n = 6$). The expression of Na^+ channels in human fibroblasts has been noted in approximately 20% of the cells, and the amount of current expressed varied widely. Na^+ current expression was not correlated with K^+ current expression nor with passage number.

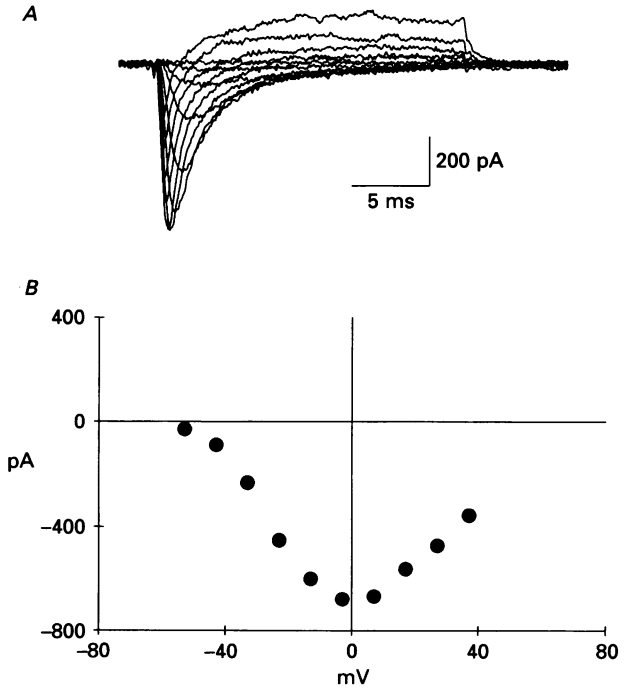

Fig. 10. 'Fast' Na^+ current. *A*, family of currents recorded in response to an identical pulse stimulation protocol as the Na^+ current shown in Fig. 8. This recording was with standard potassium aspartate in the pipette. Note that the rate of inactivation is faster than the current illustrated in Fig. 8. *B*, current–voltage relation obtained from the peaks of the pulses shown above.

As with the K^+ currents, a subtype of Na^+ current was observed. Figure 10 shows what is here termed 'fast' Na^+ current. The time to peak and the rate of inactivation are both faster than the 'typical' Na^+ current shown in Fig. 9. Although the kinetics during the pulse are different, the *I–V* relation (Fig. 10*B*) is very similar. This current is also abolished when the external Na^+ is replaced with TMA^+ or NMG^+ and is blocked by TTX.

Comparison of two kinetic properties between these two types of Na^+ currents is shown in Fig. 11. The rate of inactivation of the 'fast' Na^+ current is faster than the 'typical' Na^+ current at all voltages (Fig. 11*A*). The variability of inactivation time constant–voltage curves was higher in cells expressing 'typical' Na^+ current than for cells expressing 'fast' Na^+ current (data not shown). Another characteristic of Na^+ current is the steady-state inactivation–voltage curve (h_∞). The data comparing 'fast' with 'typical' are shown in Fig. 11*B*. The h_∞ curve for 'typical' Na^+ current

(triangles) shows a subpopulation (about 60%) of current which resists inactivation, seen as a shift to the right along the voltage axis.

Ca^{2+} channels

Using standard potassium aspartate in the pipette and mammalian Ringer solution in the bath, no inward currents consistent with Ca^{2+} channels were observed.

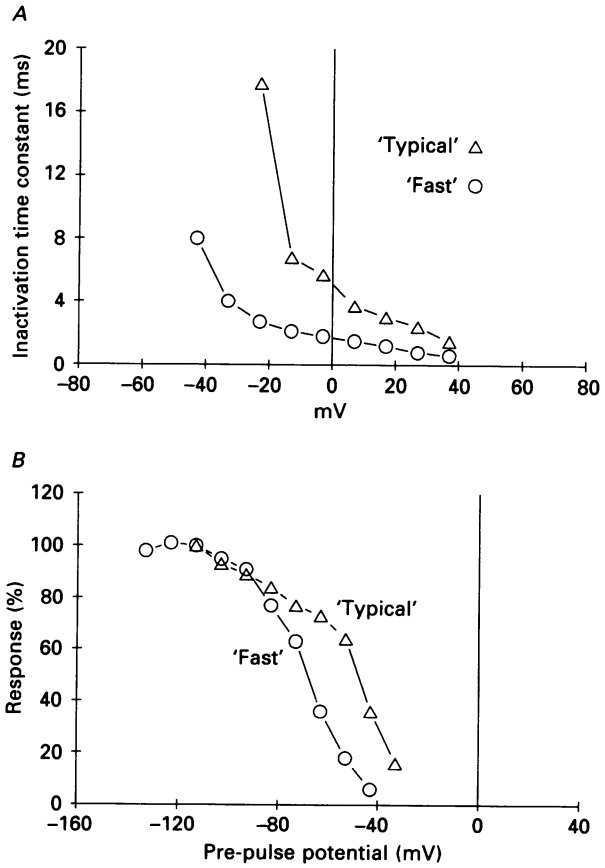

Fig. 11. Comparison of 'typical' and 'fast' Na^+ current. *A*, single exponential fits of the time constant of the falling phase of the Na^+ currents are shown for both 'typical' and 'fast' subtypes. The inactivation time constants are slower at all potentials for the 'Typical' Na^+ current. Data obtained from sweeps shown in Figs 8 and 10. *B*, steady-state inactivation curves (h_∞) are generated by normalizing the Na^+ current measured during a pulse to 17 mV which had been preceded by a 50 ms pulse at the potential plotted. This pulse protocol had been performed on the same cells shown in Figs 8 and 10. Note that the 'typical' Na^+ current seems to express a population of channels whose inactivation is shifted to potentials about 20 mV more depolarized than the 'fast' Na^+ channels.

However, voltage-dependent Ca^{2+} channels similar to those found in 3T3 cells have also been reported to occur in human fibroblasts (Chen, Corbley, Roberts & Hess, 1988). Ca^{2+} channels are known to require optimized recording conditions for maintenance and measurement of their currents. To look for voltage-dependent Ca^{2+}

currents, a pipette solution consisting of caesium aspartate with added ATP was used, along with replacing the extracellular solution with isotonic Ba^{2+}. When recording with these conditions, inward currents suggestive of Ca^{2+} channels were sometimes seen (Fig. 12). The frequency of observing Ba^{2+} currents was lower than

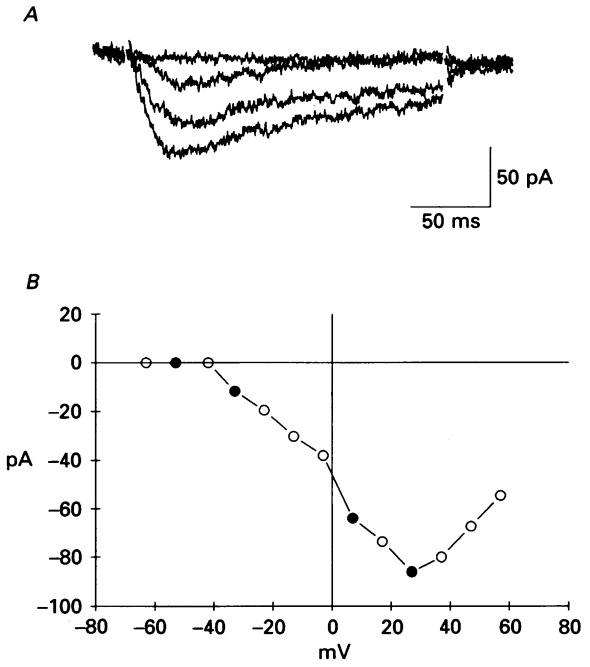

Fig. 12. Voltage-dependent Ca^{2+} current. *A*, whole cell currents measured in response to 200 ms depolarizing pulses from a −93 mV holding potential. The pipette solution was caesium aspartate to which 4 mM-ATP had been added. The bath solution was isotonic Ba^{2+} Ringer solution. Linear transients were subtracted using a P/4 protocol. *B*, peak-current–voltage curve measured from the data in part *A*. ●, traces displayed in part *A*.

10% (two of twenty-four cells) suggesting that the expression of Ca^{2+} channels is not constitutive in human fibroblasts.

Voltage-independent channels

Cl^- channels

An osmotically activated Cl^- current in lymphocytes has recently been reported (Cahalan & Lewis, 1988). As seen in Fig. 13, when fibroblasts were exposed to hypotonic solutions, an outwardly rectifying current with a reversal potential near −60 mV is induced. This modulation is probably ATP dependent because this current washed out if there were no added nucleotides in the pipette solution as described in lymphocytes (Cahalan & Lewis, 1988). In contrast, the response to decreased osmolarity was larger and the kinetics of the response were faster if ATP was included in the pipette solution (Fig. 13*B*). The induction of Cl^- current occurred in every cell in which ATP was included in the pipette solution, suggesting that this current is normally expressed and can be activated by osmotic stimulation. Ion

substitution experiments were performed (Fig. 14) by replacing the external Cl^- with organic anions such as aspartate or propionate. The Cl^- current was greatly reduced in the presence of the large organic anions, showing that the current is Cl^- selective.

Gap junctions and 'K^+ leak'

A voltage-independent K^+ current was consistently seen in cells that had formed cell-to-cell contacts. Figure 15 illustrates the differences between cells recorded

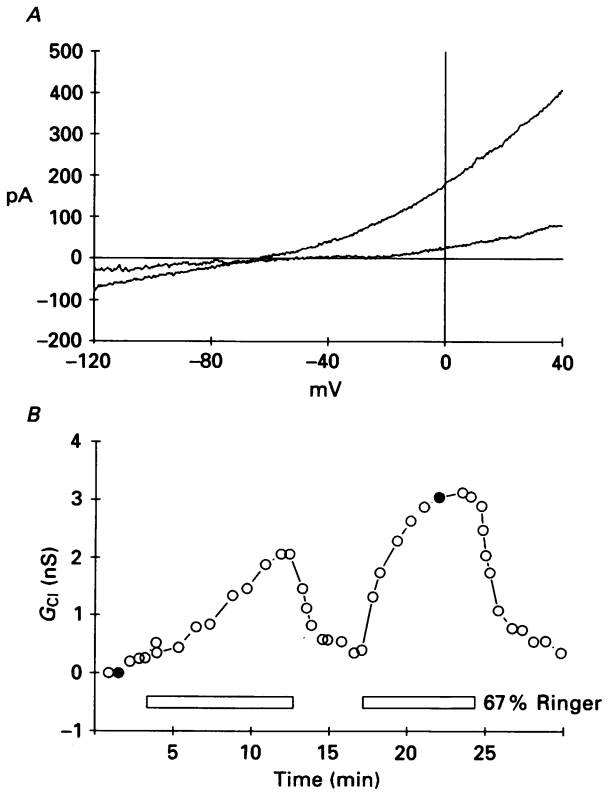

Fig. 13. Osmotically activated Cl^- current. *A*, whole-cell ramp currents measured before and during 2/3 strength Ringer solution application. The pipette solution was potassium aspartate to which 0·3 mM-GTP had been added. Note the outward rectification characteristic of the induced current. *B*, slope conductance between −40 and +40 mV (G_{Cl}) has been plotted *vs.* time after initiation of whole cell. The periods during which the hypo-osmotic stimulus was applied are indicated by the boxes along the bottom of the graph. ●, sweeps shown in part *A*.

during and after removing cell-to-cell contact. While the cell is in contact with neighbouring cells, a linear current reversing near −80 mV is seen. The capacity transient during the small test pulse shows a low cell input resistance (200 Ω) and high membrane capacitance (90 pF). After the cell is pulled off the dish, breaking

contact with the dish and with other cells, the cell input resistance increases (3 Ω) and the capacitance drops to a value typical of single fibroblasts (30 pF). The change in capacitance clearly shows that fibroblasts exhibit electrical coupling consistent with communication through gap junctions.

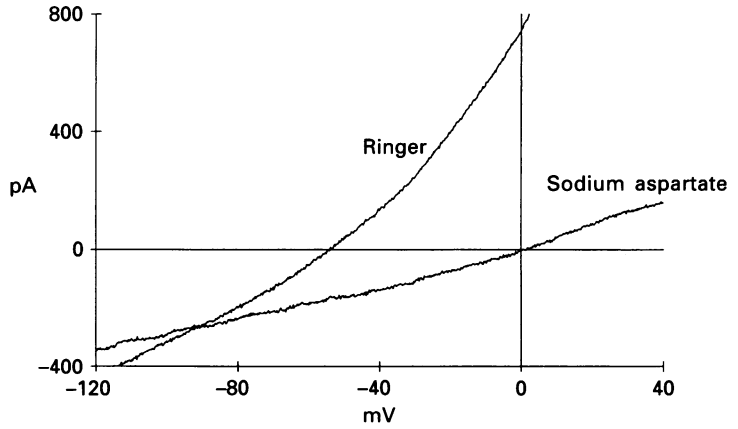

Fig. 14. Ion substitution on Cl^- current. Whole-cell ramp responses of a cell whose pipette solution was measured to have an osmolarity of 420 mosmol. After steady induction of the Cl^- current had been obtained, the mammalian Ringer solution was exchanged with a sodium aspartate Ringer solution. The sweeps were corrected for junction potential shifts.

Ion substitution experiments were performed to determine the ion selectivity of this current. When the extracellular $[K^+]$ concentration was raised (Fig. 16) the reversal potential of the current shifted as predicted by the Nernst potential, suggesting a high selectivity for K^+ over Na^+. Substitution of choline for Na^+ (Fig. 16) resulted in very little change indicating low permeability for Na^+. There was a very tight correlation of this current's expression and the existence of cell-to-cell contact. In addition, the amount of 'K^+ leak' conductance was roughly proportional to the number of cells that were in contact with the clamped cell (compare Figs 15 and 17).

The dependence of this 'K^+ leak' current on cell–cell contact was investigated by methods to measure the current in the same cell with and without contact. With human fibroblasts, it was possible to isolate the cell from its neighbours by slowly pulling the cell off the dish using the mechanically stable gigaohm seal. The other method used, which did not disrupt the cell–substrate contacts, was to ablate the neighbouring cells with a second pipette. The results described occurred using either method to isolate cells, suggesting that cell–substrate interactions are not regulating the 'K^+ leak' current.

Since the fibroblasts are electrically coupled through gap junctions, one explanation for the observed K^+ leak could be that it consists of the summed activity of K^+ leak from many individual cells. The experiment illustrated in Fig. 17, however, suggests that this interpretation may be too simplistic. Cell pairs were chosen and recording was begun on one member of the pair. After recording the K^+

leak, the other member of the pair was ablated and K^+ leak was recorded from the remaining cell. The K^+ leak before ablation is about four times as large as the K^+ leak after ablation, inconsistent with a simple summation hypothesis.

Patterns of ion channel expression

Cell parameters and voltage-dependent K^+ current expression

Isolated cells can vary over a wide range in capacitance from 10 to 50 pF with an average of 25 pF. The input resistance of the isolated cell is typically in the range of

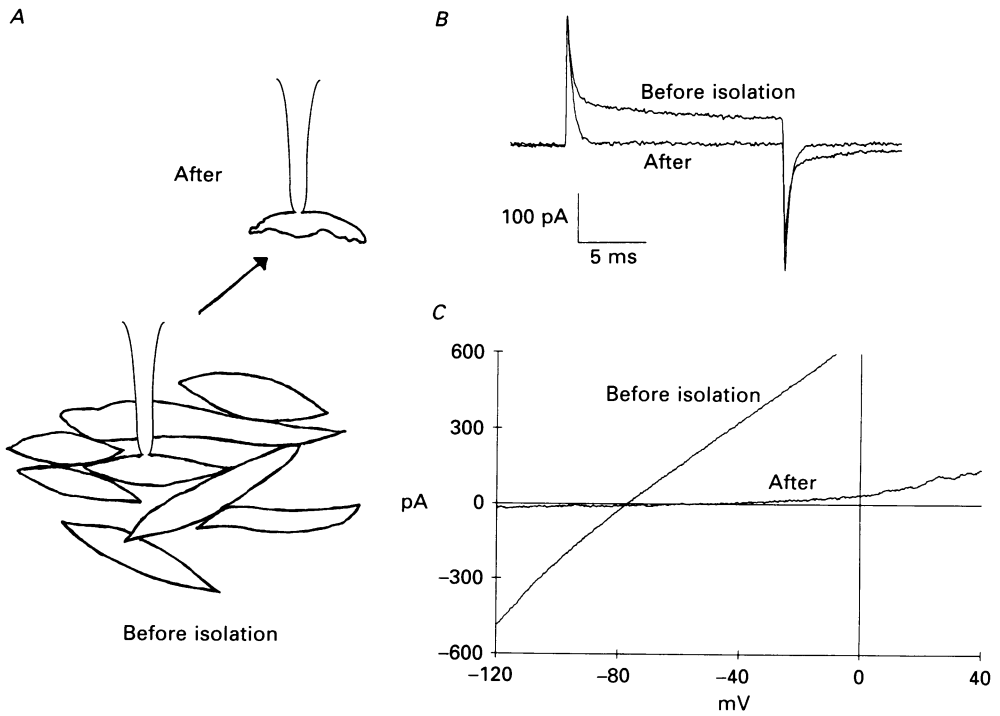

Fig. 15. Cell–cell contact associated 'K^+ leak'. *A*, cartoon illustrating cell–cell contact and the isolation of the monitored cell by pulling it off the dish and breaking all contacts with neighbouring cells. *B*, the response to a small test pulse illustrating the capacity transients measured before and after isolation. Quantification of C_m by integrating under the curves gives values of 90 pF before and 30 pF after isolation. Note the additional time constants of decay which indicate charging of neighbouring cells membranes. *C*, ramp currents recorded in the whole-cell configuration before and after isolation of the cell. The currents in the cell before isolation clearly show an additional linear current whose reversal potential is near 80 mV, the potential expected for a K^+-selective current. The sweep after isolation shows very little current of this type.

1–20 Ω. Simply pooling all the voltage-dependent K^+ currents and scoring all cells with outward rectification above −20 mV, about 60% of the cells expressed some sort of K^+ current. There were two conditions in which the percentage of cells expressing K^+ current decreased: when the cells were reaching high passage numbers (passage 13 or higher) and were beginning to senesce, or if they were serum deprived

for at least 12 h prior to recording. Over the range of passage number values from 6 to 12, the percentage of cells expressing K^+ current is relatively stable at about 70%, while the percentage is much lower for cells of higher passage number.

Ion channel expression is independently regulated

During the course of these experiments, many combinations of the ion channels described here were found to be co-expressed. The frequency of these occurrences is

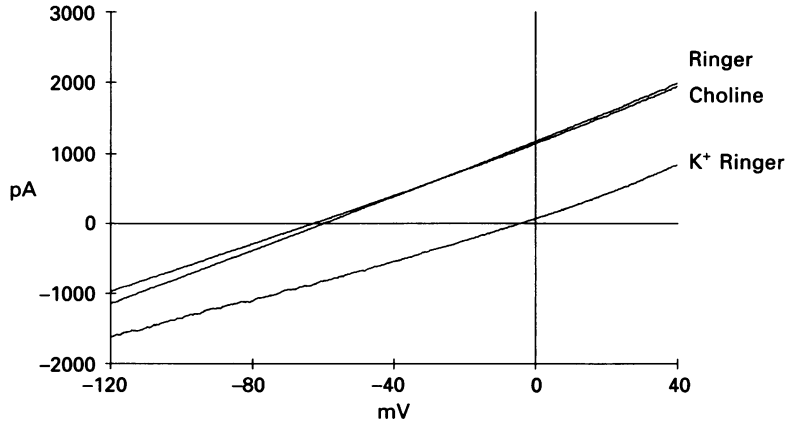

Fig. 16. Ionic dependence of K^+ leak. Ion substitution experiments on the cell–cell contact associated 'K^+ leak' are consistent with a high selectivity for potassium. The pipette contained standard potassium aspartate. Exchange of mammalian Ringer solution with K^+ Ringer solution causes a shift in reversal potential to near 0 mV. This shift is reversed when the bath is returned to mammalian Ringer solution. Substitution of the Na^+ with choline Ringer solution caused very little shift in the reversal potential.

about what one would expect from the combined probability of observing each current by itself. This argues against a hypothesis which links the expression of one current to expression of others, e.g. voltage-dependent Na^+ currents might only be seen when voltage-dependent K^+ currents are also expressed.

Empirical observations

During the course of these experiments, it has been necessary to change the manufacturer or lot number of serum. These transitions have sometimes been marked by qualitative changes in the expression of ion channels. For instance cells that were consistently expressing large amounts of K^+ current suddenly shifted to low level expression. In another case, a robust stimulated modulation of an ion current became barely observable. These observations emphasize the point that serum is an incompletely defined component of growth medium and that human fibroblasts can be sensitive to changes in the spectrum of growth regulatory substances contained in serum. Attempts to grow cells in serum-free defined medium were made but were discontinued for the following reasons: (1) the cells adapted poorly, (2) the percentage of cells expressing voltage-dependent currents was very small, similar to behaviour of serum-deprived cells, and (3) the manufacturers of serum-defined media, for proprietary reasons, would not disclose the medium components.

DISCUSSION

Diversity of ion channels expressed

Multiple kinds of K^+ channels

The number of K^+ channels documented in the literature increases yearly. Frequently a cell type expresses multiple types of K^+ channels at the same time (French & Stockbridge, 1988; Hoshi & Aldrich, 1988), which can be distinguished by

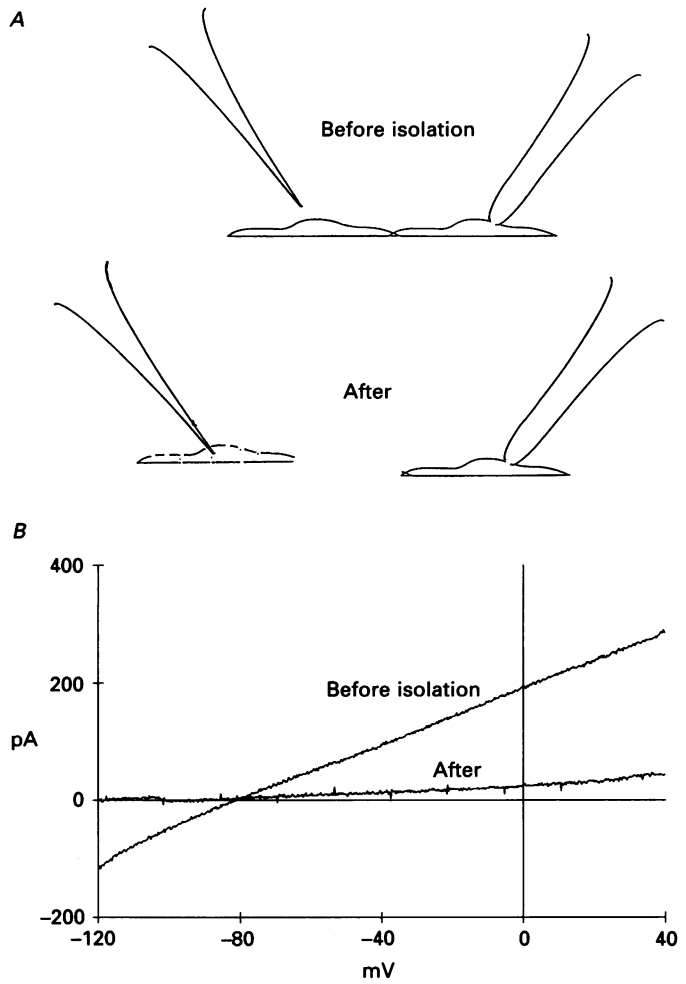

Fig. 17. Cell–cell contact-associated K^+ current. *A*, cartoon illustrating experiment where cell pairs were found and the amount of 'K^+ leak' measured. An additional pipette is then used to ablate the distal cell, breaking all contact with the cell being monitored without significantly changing its morphology. *B*, ramps obtained before and after distal cell ablation showing the dependence on cell–cell contact for expression of the 'K^+ leak' current. Note also that the 'K^+ leak' current seems more than halved after ablation, suggesting against the trivial explanation that this current is a simple cell-mediated K^+ leak.

differences in gating kinetics or pharmacology. In human fibroblasts, at least two voltage-dependent K^+ channels are present, as well as an inward rectifier K^+ channel, and a 'maxi-K' Ca^{2+}-activated K^+ channel. The different voltage-dependent K^+ channels were identified in cells which seemed to express only a single kinetic type of K^+ current. Attempts to isolate these currents with pulse protocols or with pharmacological agents such as TEA, 4-AP, CTX and apamin worked poorly. Thus there may be multiple K^+ channel types underlying the observed currents. Indeed, more than ten types of single channels were observed which differed by size or by gating properties (data not shown); thus single-channel data have not been assigned to each subtype of K^+ current.

Other voltage-dependent channels

The expression of Na^+ or Ca^{2+}channels is often described as a marker for excitable cells. As more non-excitable cells are studied, however, it has become apparent that they are capable of expressing Na^+ and Ca^{2+} channels similar to those of excitable cells (Lombet *et al.* 1982; Chen *et al.* 1988). The present study shows that Na^+ currents found in human fibroblasts differ in kinetics and TTX sensitivity from Na^+ currents expressed in neuronal cells. The 'typical' Na^+ current may be composed of at least two populations of Na^+ channels as evidenced by the multicomponent h_∞ relation. Fibroblast Na^+ channels may be more similar to those described in muscle or cardiac tissue (Kirsch & Brown, 1989). Alternatively, human skin fibroblasts might not process the neural form of the Na^+ channel correctly.

Voltage-independent channels

The finding of a K^+-selective conductance which is correlated with cell-to-cell contact has not been reported. This may be due to the routine practice of only recording from isolated cells. Another reason may be that this current was dismissed as being due to the summed K^+ leak of individual cells. The seeming lack of any observable 'K leak' current in isolated cells suggests that the current is somehow gated in response to formation of cell–cell contacts. The correlation is strongest with the existence of functionally open gap junctions, suggesting some association between gap junctions and a voltage-independent K^+ conductance. One possibility could be that all cells express 'K^+ leak' whose activity depends on a diffusible factor which dialyses away in whole cell but does not pass through gap junctions. A patch-clamp study in mouse L cells (Hosoi & Slayman, 1985) suggested that the resting membrane conductance is K^+ dominated which decayed over a period of minutes. An interesting hypothesis to consider, however, is the possibility that the establishment of open gap junctions between cells causes the formation of voltage-independent K^+ channels.

Possible regulation of ion channel expression

The variability seen in voltage-dependent K^+ current expression is correlated with growth state. Reduced expression of K^+ current was seen after serum withdrawal and a similar phenotype was seen as the cells entered senescence. One possible explanation for reduced expression is that K^+ channels are expressed only during certain phases

of the cell cycle. Cell populations in log growth will be in all phases of the cell cycle and the percentage of cells which show K^+ channel expression would (assuming random cell selection) reflect the proportion of the cycle in which K^+ channel expression occurs. Cells in reduced serum tend to arrest at the G0/G1 boundary, and at this point would be predicted to have reduced K^+ channel expression. Up regulation of K^+ channels during a proliferative phase has been reported for lymphocytes (DeCoursey, Chandy, Gupta & Cahalan, 1987).

An alternate explanation is that expression of K^+ channels is influenced by environmental signals. This was supported by the observation of abrupt changes in the patterns of ion channels expressed when serum lots were switched. The relative balance of growth factors may favour certain ion channel phenotypes over others.

Overall, however, the diversity of ion channel phenotypes seen suggests that voltage-dependent ion channel expression is not tightly regulated. The large number of channel types expressed seems more comprehensible as a 'leaky' expression of ion channels by human skin fibroblasts in culture. Clear evidence of ion channel regulation will probably await better defined medium formulations in which studies concerning changes due to the effects of varying a single growth modulatory factor at a time can be undertaken.

Possible roles for the ion channels found

The maintenance of the extracellular matrix (ECM) would require secretion of both degradation enzymes and later of new ECM material. Ion channels have been suggested to have roles in both the exocytosis and endocytosis processes. L cells have increased activity of Ca^{2+}-activated K^+ currents during stimulated phagocytosis (Okada *et al.* 1981). Mast cells express a cation channel which is associated with degranulation (Penner, Matthews & Neher, 1988).

Ion channels may be involved in motility. The mobilization of fibroblasts to infiltrate a wound site suggests a stimulated chemotactic motility. Subconfluent fibroblasts often show morphologies consistent with ruffling membrane, which is associated with cell motility. Injection of quiescent fibroblasts with activated *ras* oncogene proteins stimulates ruffling of the membrane (Bar-Sagi & Feramisco, 1986). Contractile elements involved in motility are dependent on Ca^{2+} and a plasma membrane Ca^{2+} flux could be involved. It might be possible to correlate ion channels with motility using human fibroblasts.

Once the fibroblast gets to the wound site, it may experience changes in the osmotic strength of its surroundings. The ability to volume regulate has been studied in lymphocytes and is probably common to all mammalian cells. In lymphocytes, the regulatory volume decrease seen in response to hypotonic solutions is dependent on a rise in both Cl^- and K^+ permeability (Cheung, Grinstein, Dosch & Gelfand, 1982). As both of these ions exit the cell down their concentration gradients, the loss of solutes causes a loss of intracellular water. The mechanism underlying the ATP dependence of this current has not been elucidated.

Perhaps the most interesting possibility to consider is that some of the ion channels expressed in the fibroblast are involved in signalling mechanisms analogous to the role of ion channels in excitable tissues. As is shown in the companion paper (Estacion, 1991), ion channels may be involved in the signal transduction response

of human fibroblasts to a specific peptide mitogen. The possibility exists that different ion channels are involved depending on whether the signal codes for proliferation or for an action such as secretion. Understanding the roles of the ion channels expressed in human fibroblasts may lead to better understanding of human diseases.

I would like to thank Dr Michael Cahalan for his support and guidance while I was a member of his laboratory. I would also like to thank Ruth Davis for help with cell culture. This work was supported by NIH grant NS14609.

REFERENCES

ADRIAN, R. H. & FREYGANG, W. H. (1962). The potassium and chloride conductance of frog muscle membrane. *Journal of Physiology* **163**, 61–103.

ARMSTRONG, C. M. & BEZANILLA, F. (1974). Charge movement associated with the opening and closing of the activation gates of the Na channels. *Journal of General Physiology* **63**, 533–552.

BAR-SAGI, D. & FERAMISCO, J. R. (1986). Induction of membrane ruffling and fluid-phase pinocytosis in quiescent fibroblasts by ras proteins. *Science* **233**, 1061–1068.

CAHALAN, M. D. & LEWIS, R. S. (1988). Role of potassium and chloride channels in volume regulation by T lymphocytes. In *Cell Physiology of Blood*. Rockefeller University Press, New York.

CHEN, C., CORBLEY, M. J., ROBERTS, T. M. & HESS, P. (1988). Voltage-sensitive calcium channels in normal and transformed 3T3 fibroblasts. *Science* **239**, 1024–1026.

CHEUNG, R. K., GRINSTEIN, S., DOSCH, H. M. & GELFAND, E. W. (1982). Volume regulation by human lymphocytes: characterization of the ionic basis for regulatory volume decrease. *Journal of Cellular Physiology* **112**, 189–196.

CONNOR, J. A. & STEVENS, C. F. (1971). Voltage clamp studies of a transient outward membrane current in gastropod neural somata. *Journal of Physiology* **213**, 21–30.

DECOURSEY, T. E., CHANDY, K. G., GUPTA, S. & CAHALAN, M. D. (1987). Mitogen induction of ion channels in murine T lymphocytes. *Journal of General Physiology* **89**, 405–420.

ESTACION, M. (1991). Acute electrophysiological responses of bradykinin-stimulated human fibroblasts. *Journal of Physiology* **436**, 603–620.

FRENCH, A. S. & STOCKBRIDGE, L. L. (1988). Potassium channels in human and avian fibroblasts. *Proceedings of the Royal Society* B **232**, 395–412.

HAMILL, O. P., MARTY, A., NEHER, E., SAKMANN, B. & SIGWORTH, F. J. (1981). Improved patch-clamp techniques for high-resolution current recording from cells and cell-free membrane patches. *Pflügers Archiv* **391**, 85–100.

HOSHI, T. & ALDRICH, R. W. (1988). Voltage-dependent K^+ currents and underlying single K^+ channels in pheochromocytoma cells. *Journal of General Physiology* **91**, 73–106.

HOSOI, S. & SLAYMAN, C. L. (1985). Membrane voltage, resistance, and channel switching in isolated mouse fibroblasts (L cells): A patch-electrode analysis. *Journal of Physiology* **367**, 267–290.

INCE, C., LEIJH, P. C. J., MEIJER, J., VANBAVEL, E. & YPEY, D. L. (1984). Oscillatory hyperpolarizations and resting membrane potentials of mouse fibroblast and macrophage cell lines. *Journal of Physiology* **352**, 625–635.

KIRSCH, G. E. & BROWN, A. M. (1989). Kinetic properties of single sodium channels in rat heart and rat brain. *Journal of General Physiology* **93**, 85–99.

LAMB, J. F. & MACKINNON, M. G. A. (1971). The membrane potential and permeabilities of the L cell membrane to Na, K and chloride. *Journal of Physiology* **213**, 683–689.

LOMBET, A., FRELIN, C., RENAUD, J. & LAZDUNSKI, M. (1982). Na^+ channels with binding sites of high and low affinity for tetrodotoxin in different excitable and non-excitable cells. *European Journal of Biochemistry* **124**, 199–203.

MUNSON, R., WESTERMARK, B. & GLASER, L. (1979). Tetrodotoxin-sensitive sodium channels in normal human fibroblasts and normal human glia-like cells. *Proceedings of the National Academy of Sciences of the USA* **76**, 6425–6429.

OKADA, Y., TSUCHIYA, W., YADA, T., YANO, J. & YAWO, H. (1981). Phagocytic activity and hyperpolarizing responses in L-strain mouse fibroblasts. *Journal of Physiology* **313**, 101–119.

PENNER, R., MATTHEWS, G. & NEHER, E. (1988). Regulation of calcium influx by second messengers in rat mast cells. *Nature* **334**, 499–504.

YEN-CHOW, Y. C., CHOW, S. Y., JEE, W. S. S. & WOODBURY, D. M. (1984). Membrane potentials, electrolyte contents, cell pH, and some enzyme activities of fibroblasts. *In Vitro* **20**, 677–684.